OPEN ACCESS

ACTA METALLURGICA SLOVACA

2020, VOL. 26, NO. 2, 37-41

RESEARCH PAPER

THE CORROSION AND WEAR RESISTANCE OF LASER AND MAG WELD DEPOSITS

Anna Guzanová[1], Miroslav Džupon[2], Dagmar Draganovská[1], Janette Brezinová[1], Ján Viňáš[1], Denis Cmorej[1], Erik Janoško[1], Pavlo Maruschak[3]*

[1]Technical University of Košice, Faculty of Mechanical Engineering, Košice, Slovakia

[2]Slovak Academy of Sciences, Institute of Materials Research, Košice, Slovakia

[3]Ternopil Ivan Puluj National Technical University, Faculty of Applied Information Technologies and Electrical Engineering, Ternopil', Ukraine

*Corresponding author: anna.guzanova@tuke.sk, tel.: +421949186308, Faculty of Mechanical Engineering / Technical University of Košice, 042 00 Košice, Slovakia

Received: 20.05.2020
Accepted: 30.05.2020

ABSTRACT

The paper focuses on the possibility of HPDC molds restoration for aluminium casting by laser and MAG weld cladding with a welding wire of the same grade like the base material. A chemical analysis of the weld deposits showed a decrease in the content of some elements in the MAG deposit due to the higher thermal input to the weld bath. The lower heat input of laser welding has resulted in a higher incidence of fusion defects lack between the weld deposit and the base material. Thermal conditions during welding affected hardness of weld deposits and their abrasive resistance as well. The resistance of materials against dissolution when immersed in AlSi8Cu3 alloy was similar for both deposits and the base metal.

Keywords: HPDC; mold; immersion test; linear polarisation; abrasive wear test

INTRODUCTION

The production of molds for HPDC (a high pressure die casting) is the largest investment in a mass production of castings. Its return is closely related to its lifetime. Wear of hot working steels used for mold and dies production has stimulated many research activities. Jhavar [1] analyzed in detail the causes of dies and molds failure, while Anderson [2] conducted a similar study for extrusion tools and moreover Ebara [3] and Chander [4] for forging dies. Subsequently Markežič [5] focused on the HPDC process and considered the main mechanisms of mold failure: soldering (or die sticking), corrosion, erosion, thermal fatigue and cracking. Soldering is the bonding of the cast material to the mold surface and is the result of simultaneous metallurgical and mechanical bonding. Corrosion is associated with the loss of mold material due to metallurgical processes - especially metallurgical sticking and dissolution of the mold material by processed melt. Erosion is also characterized by the loss of material from the mold, but it is caused only mechanically - by flow of the melt in the mold [6]. The intensity of erosion increases with the mold temperature. The combination of high temperatures and pressures in the mold leads to thermal cracking of the mold material where the maximum mold temperature as well as the heating/cooling rate of the individual casting cycles play an important role [7]. Such a thermal load regime of the mold insert can also lead to oxidation of the surface layers and change of the microstructure [8] and hence the microhardness of the mold insert surface. According to Markežič [5], an adequate hardness of the mold functional surface is an essential characteristic that helps prevent the initiation and spread of wear and damage mechanisms. Subsequently, suitable technologies for the mold renovation were sought - local refilling of the material, which is missing after part deep removal of the material with cracks. In addition to the cold spraying technology tested by Lee [9] and showing promising results - the restored layer had a higher wear resistance than the original material, Chen [10] considers weld cladding to be undoubtedly the dominant restoration technology. For this purpose, for example Brezinova [11-13] tested with good results, CMT welding technology, or classic arc technologies [14-17], which are characterized by a high heat input produced in the weld bead and relatively a large volume of deposited metal. In order to minimize preheating and post-welding heat treatment, a multi-layer deposition is recommended for arc technologies, with the next layer providing heat treatment to the previous layer [15]. The relatively wide HAZ caused a great affection of the base material, and since according to Borrego [18] in the case of tensile residual stresses present in the deposit, the deposit could be just weaker point of the restored mold, the attention was next redirected to hybrid technologies [17] and technologies with a lower thermal input, in particular laser welding [18-25]. Laser welding allows, according to Borrego [18] and Cong [21,22], to achieve a smaller change in a chemical composition around the deposit, narrow HAZ, very precise deposition of a small volume of the filler material at a specified location without distortion. However, laser welding also has drawbacks. Borrego [18] notes that laser deposit can be at risk of tensile residual stresses, especially if it is single-layered [19] and planar defects, which can become cracks initiation sites. Vundru [19] in addition notes multilayer weld deposits have a high probability of compressive overall residual stresses which will improve their fatigue resistance.

Other ways of increasing the fatigue life of laser cladding are also being sought. Cong [21] tested positively the effect of biomimetic laser remelting on the fatigue life of laser cladding, and in [22] also tested the surface remelting with a certain pattern laser. Positive results are attributed to grain refinement and martensite formation at the melting point, which increases the hardness and resistance of the weld deposit to cracks propagation. Weld deposits, after machining, also requires to be coated by thin coatings which according to Knotek [26] can increase the life of the mold up to three times. Ch. Chen [10] emphasizes the need to predict the service life of restored mold parts which could help in making decision whether it is effective to proceed with a mold restoration.

The aim of this work is to determine the quality of the renovation layers created by laser and MAG welding using the same base and additive material (Uddeholm Dievar) in terms of chemical composition, continuity between the base material and weld clad, hardness, corrosion properties and change of the Young's modulus near the surface after corrosion exposition.

MATERIAL AND METHODS

Base material (BM)

Base material – Uddeholm Dievar is a high performance Cr-Mo-V alloyed hot work tool steel, which offers a very good resistance to a high temperature tempering, gross cracking, hot wear and plastic deformation. The chemical composition given by steel producer: 0.35 % C, 0.2 % Si, 0.5 % Mn, 5 % Cr, 2.3 % Mo, 0.6 % V.

Weld deposition

Three-layer weld depositions by laser and MAG welding with a wire electrode of 1 mm in diameter made of the same steel Dievar were performed under following welding conditions:

Laser welding (TruDisk 4002)
- laser power 1.8 kW
- welding speed 10 mm/s
- focusing +6 mm above base material
- wire feed speed 0.7 m/min
- protective gas Ar 4.6 (30 l/min)
- optic cable diameter 0.4 mm

MAG welding (Kemppi)
- current 180 A
- voltage 25 V
- welding speed 5.7 m/min
- protective gas: 18% CO_2 + 82%Ar (M21 STN EN ISO 14175)
- gas flow rate: 14 l/min

Chemical analysis of materials

The test specimens with weld deposit were subjected to a chemical analysis by a spark optical emission spectrometer Belec Compact Port. The chemical analysis was performed three times on the base material, welding wire and also on the weld deposit.

Metallographic analysis of materials

A test samples were cut from the deposits and used for identification of the microstructure, corrosion resistance and hardness. Samples were metallographically processed and etched by 2% Nital and Cor etching agent (120 ml CH_3COOH, 20 ml HCl, 3 g picric acid, 144 ml CH_3OH).

Measurement of hardness

The microhardness of the base material and weld deposits were measured on Shimadzu HMV-2 along by three parallel lines in constant spacing across the sample thickness including weld deposit, HAZ, and base material. Load force applied was 980.7 mN (HV0.1), time 15 s.

Linear polarisation method

The corrosion properties of the base material and the weld deposit were determined using a linear polarization method with a three-electrode connection – weld deposit/base material, saturated calomel electrode and platinum electrode in 3.5% NaCl solution. The material OCP was measured in the unloaded circuit within 30 minutes, followed by polarization to the cathodic and anodic region ± 250 mV. Tafel curves have been further analysed with aim to determine r_{corr}.

Hot-dip corrosion test by immersion in molten metal

The dissolution of the base material and the deposits in processed melt was tested by immersion test. The ground and polished specimens of the base material and weld deposits were exposed in an AlSi8Cu3 alloy melt at a temperature of 680 ± 20°C for 300 minutes. The dissolution rate was identified by measuring the thickness of the compact layer of dissolution products.

Abrasive wear test

An abrasive wear was determined by the relative movement of the material relative to the abrasive cloth with grit size of P80 and P120 under load of 19.62 N (2 kg) and wear track was 40 m. The test was performed three times for each - base material, MAG and a laser weld deposition. A fresh abrasive cloth was used for each test.

RESULTS AND DISCUSSION

Chemical analysis of materials

Table 1 shows the chemical analysis of the base material, welding wire and the deposits as the average of the three measurements.

Table 1 The chemical analysis of the base material, wire and weld deposits, wt. %, Fe – balance, P<0.002, S=0.004

	C	Si	Mn	Cu	Al	Cr	Mo	Ni	V
BM	0.457	0.18	0.40	0.07	0.02	4.98	2.04	0.09	0.72
wire	0.362	0.16	0.37	0.05	0.02	4.14	3.73	0.35	0.09
laser	0.445	0.20	0.28	0.40	0.01	4.58	2.19	0.08	0.76
MAG	0.338	0.13	0.26	0.53	<0.002	4.36	2.04	0.07	0.52

The change in the content of the individual elements in the weld over the base and filler material is due to the mixing of the base and filler material and the oxidation-reduction processes during the transfer of the molten metal in the arc. A greater loss of additive elements is observed with MAG technology due to the higher heat input to the weld area.

Metallography of weld deposits

Fig. 1 shows the macrostructure of the laser weld deposit, the microstructure of the base material, the heat affected zone and the weld deposit.

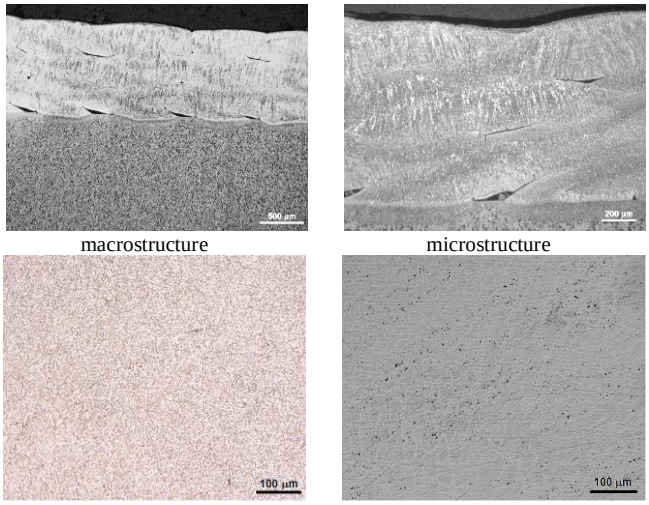

macrostructure microstructure

microstructure of BM laser weld deposit

Fig. 1 Macro- and microstructure of laser weld deposit and BM, Nital, LM

Crack defects were not observed by the light microscopy technique in the Dievar base material under 1 mm thick weld deposit. In the middle of deposit thickness, isolated microcavity defects were present. On the boundary between the weld deposit and the base material there were defects in the connection (the lack of fusion defects) of 0.50 mm average length which occasionally corresponded to the crack defects. Between the weld metal and the base material, as well as between the adjacent deposit layers, there were present the lack of fusion lenticular defects. Capello [27] also notes that the first layer in the multilayer laser cladding is critical because it provides attachment to the substrate. In the area of fusion defects lack between the base material and the weld deposit, lines of oxygen and elements present in the weld deposit were detected by a semi-quantitative EDX microanalysis. In the vicinity of the crack roots which corresponded to lack of fusion defects between the deposit and base material, only the alloying elements in the deposit were present. Defects are not of metallurgical origin as examined. The defects at the base material – a weld deposit interface and the defects between the weld deposit layers are due to the low heat input during laser welding, which was not sufficient to ensure completely remelting the previous material layer. Borrego in [18] also observed the same defects at certain welding parameters. He confirmed that these defects became initiation sites in a fatigue test, especially when the tensile residual stress acts in the deposit. It is therefore necessary to pay attention to the optimization of the welding process and to keep in balance the positives of low heat input and the risk of fusion defects lack.

Fig. 2 shows the macrostructure of the MAG weld deposit, the microstructure of the base material, the heat affected zone and the weld deposit.

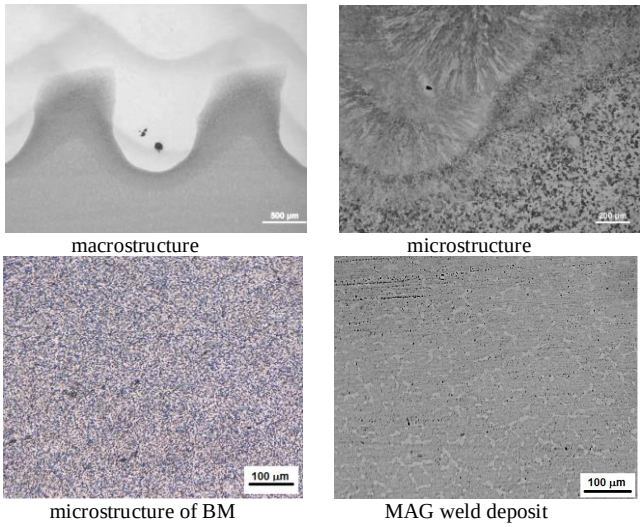

macrostructure microstructure

microstructure of BM MAG weld deposit

Fig. 2 Macro- and microstructure of MAG weld deposit and BM, Nital, LM

Crack defects were not observed by the light microscopy technique in the Dievar base material under a 2.2-3.2 mm thick weld deposit. Isolated defects – microcavities were present as a result of entrapped gas bubbles. There were observed no defects in the connection between the base material and the weld deposit, nor between the adjacent layers in deposit. No cracks were observed by light microscopy technique. This is related to the higher thermal input of MAG technology compared to laser welding technology. The microstructure of the experimental material, soft annealed, consists of carbides heterogeneously distributed in the ferritic matrix. Transition between BM and MAG deposit shows characteristic undulating pattern, observed also by Nevskii in [28] in plasma deposits. Pattern formation is ascribed to flow of an incompressible viscous fluid at deposit/BM interface and to combination of Rayleigh–Taylor and Kelvin–Helmholtz instabilities, which dominates at specific transversal velocity.

The micro- and macro-structure of the weld deposit shows the heat affection lines of the first bead by next deposited layer. Based on the work of Suarez [14], it is possible to assume a slight tempering of the first layer by next one, which could temper sudden changes in hardness across the deposit. The hardness profile of the weld deposit is given in the next chapter.

Macrodefects either in the form of lack of fusion defects or air bubbles, but also microstructural formations such as heterogeneously distributed carbides can be considered as stress concentrators, from which, at the moment when the driving forces for crack propagation exceed the stress intensity factor, cracks can propagate in the weld or in the base material. The speed of short-crack propagation depends, among other things, on the grain composition (size, orientation etc.), but also on the residual stresses present in the weld. Although the presence of compressive residual stresses is generally considered to be positive, Gliha [29] states that at the stress levels much lower than the fatigue limit, a short crack begins to propagate through the field of compressive residual stresses. Due to the decreasing compressive residual stress during the crack propagation, the crack closure decreases and effective stress intensity factor increases. The result is the quickly increasing short-crack propagation. Despite the decelerated initial crack propagation due to the compressive residual-stress field, the crack, sooner or later, propagates to the domain of the tensile residual stress. Then the crack propagates faster.

Microhardness of weld deposits

Fig. 3 shows course of microhardness from weld deposit made by both technologies through HAZ to base material.

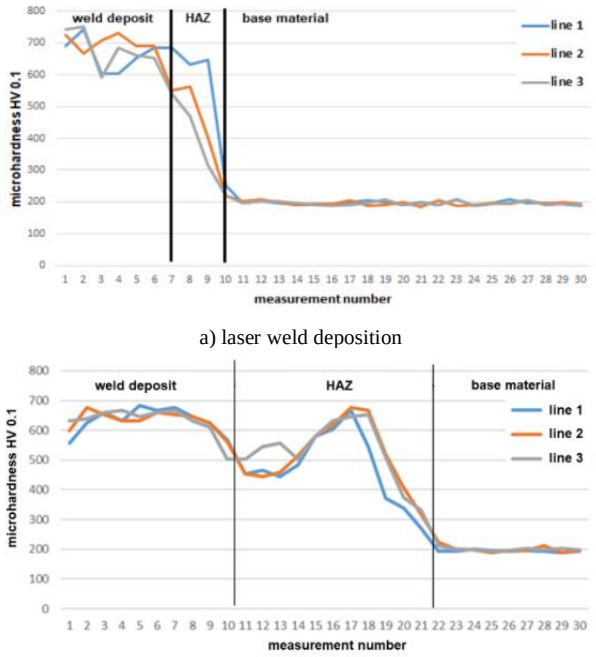

a) laser weld deposition

b) MAG weld deposition

Fig. 3 Graphic course of hardness from MAG weld deposit, through HAZ to base material

The average hardness of the base material was 195 HV0.1. The hardness of the laser deposit was highest in the top layer (680 HV 0.1), dropping sharply through the heat affected zone to the hardness of the base material. Due to the lower heat input, the HAZ area was narrower compared to the MAG technology. The course of hardness through laser cladding is similar to that found Kattire in [24] on the same material. By phase analysis he proved connection between hardness and microstructure in deposit areas. The highest hardness in top layer of deposit is caused by harder carbides distributed in the martensitic matrix. Far from the surface, their precipitation decreases to the area with less hard-type carbides located in the tempered martensite matrix.

The highest hardness was detected in the surface layer of the MAG weld deposit (670 HV 0.1). Another hardness peak was recorded again in the weld deposit however at a depth of 5-7 mm below the surface (663 HV 0.1). At a greater distance, the hardness dropped very quickly through HAZ to the hardness of the base material (197 HV0.1). Suarez in [14] attributes the peaks in the hardness of multi-weld deposits to their too short overlapping, with alternating tempered and non-tempered areas. Hu [15] notes that the first layer which is welded without preheating and hence its cooling rate is high, has a fine-grain structure and contains hardening phases, and even after the next layer deposition, tempered grain size remains still fine. The temperature of the first layer serves as the preheating for the next layer deposition, and the temperature of the entire workpiece increased continuously with the deposition of the subsequent layers. Therefore, the cooling speed decreased as well as the fraction of the hardening phases, which resulted in lower hardness. Both deposits are characterized by high surface hardness, which, according to Markežič [5], may lead to decreases in the density and depth of thermal fatigue cracks.

Corrosion resistance of materials – Tafel analysis

Table 2 shows the corrosion characteristics measured and calculated by Tafel analysis valid for the base metal - Dievar and weld deposits made by particular technologies.

Table 2 Results of Tafel analysis for Dievar

	E_{corr} [mV]	I_{corr} [µA]	bc [mV]	ba [mV]	r_{corr} [mmpy]	Rp [Ohm]
BM	-579	7.84	834	75	0.29	3311

Laser	-482	8.53	367	114	0.31	3088
MAG	-499	12.70	789	109	0.46	2739

Table 2 shows higher corrosion rate of both weld deposits compared to BM. This is a consequence of a change in the chemical composition of the weld due to melting, as the content of all important elements has been reduced, which can be seen in Table 1. The lower decarburization of the laser deposit resulted in a minimal increase in r_{corr}, while in the MAG deposit the slightly higher decarburization resulted in a more pronounced increase in the corrosion rate.

Hot-dip corrosion by immersion in Al alloy

Fig. 4 shows the results of area cross-sectional microanalysis (mapping) through the interface between the base material and melt or between welds and AlSi8Cu3 melt after 300 minutes of immersion.

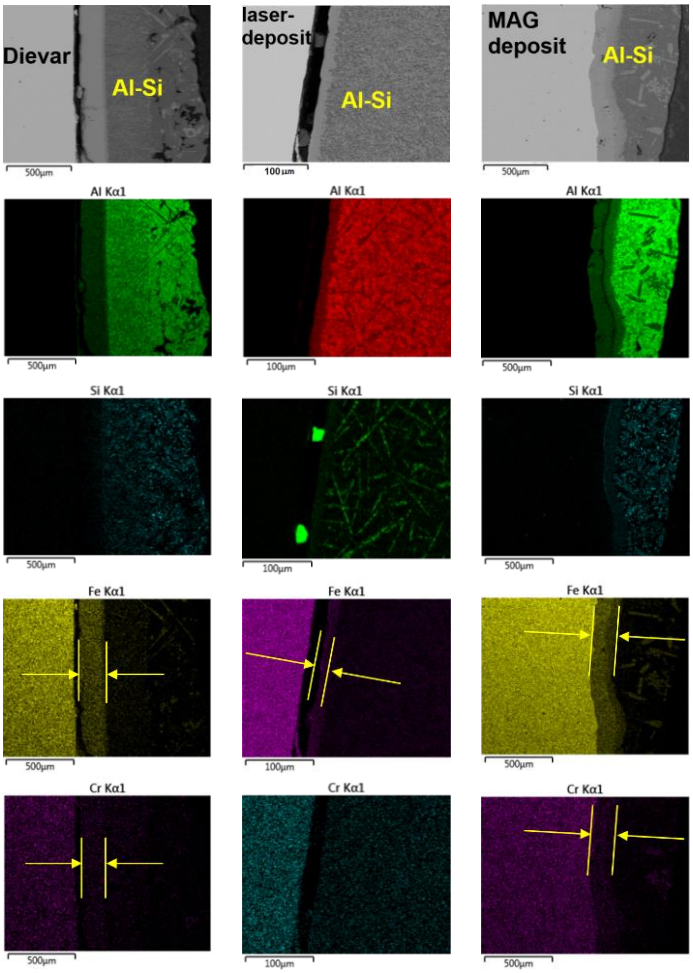

Fig. 4 EDX mapping of the base material/weld deposits interface after immersion test

For both a ground and polished test specimens after 300 minutes of exposure in the melt of an aluminum alloy, a compact layer of the dissolving products of the base material or weld deposits remained on the both surfaces of the test specimens. Its thickness was determined using cross-sections and verified by mapping, mainly by Fe and Al maps. Thickness of compact layer on base material, laser deposit and MAG deposit was 200 µm, 25 µm and 180 µm, respectively. Fe map indicates a respective dissolution of the base material/weld deposit in processed melt, whereas Al map indicates the dissolution of melt in the base material/weld deposit. It can be concluded, that resistance of the experimental weld deposits was not worse compared to hardened Dievar reference (base) material, moreover, resistance of laser deposit was noticeably higher.

Zhu [30] observed, when tested the solubility of the same steel in Al alloy's melt, the intermetallic layer that formed by consuming the base metal. Fe-Al binary diagram describes the occurrence of several intermetallic phases. The intermetallic layer is always more brittle than the original metal. Its formation also affects the mold surface properties and the relatively hard mold surface becomes more vulnerable. The dissolution products are washed away from the mold surface by a melt stream and the dissolution can continue in the next casting cycle. This phenomenon cannot be completely avoided. It is important to ensure that the resistance of weld deposits against dissolution is at least at the same level as resistance of new mold. The results confirmed such resistance.

Abrasive wear test

Fig. 5 shows the cumulative mass loss of the base material and weld deposits at two abrasive cloth grit sizes.

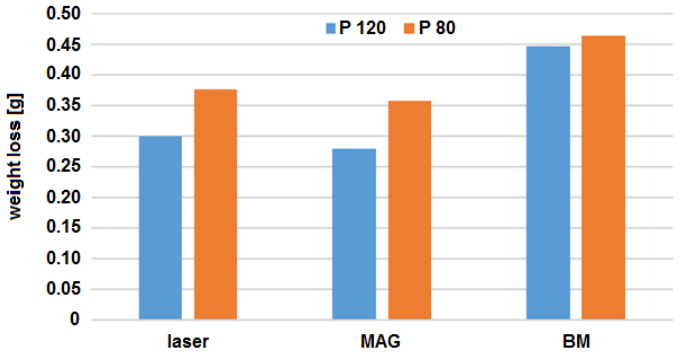

Fig. 5 Mass loss of base material and weld deposits after wear test

Fig. 5 shows a slightly higher abrasive wear resistance of weld deposits against the base material. This is in direct proportion to the higher hardness of the weld deposits compared to the base material. The abrasive cloth with a grit size P80 caused higher material removal than P120. The results of the test indicate that when restore the molds by welding with both technologies, we will obtain a layer with higher wear resistance than the original base material.

However, the wear resistance of weld deposits is related not only to their hardness, but also to the residual stresses in the weld deposits. Although monitoring of residual stresses has not been included in experimental work, current publications show that the volume expansion caused by phase changes (especially martensitic transformation) in the weld deposit during the cooling process acts against shrinkage forces in the weld deposit. Thereby tensile residual stresses in the deposit are reduced and need of deposit post treatment is partially replaced. As a result, the hardness and abrasion resistance of the deposit are improved [31].

CONCLUSIONS

The paper brought the research results of weld deposits made by laser and MAG welding technology. The results subsequently showed the importance of welding process optimization which affects the occurrence of internal defects in relevant deposits. Their presence can be manifested in fatigue characteristics. Due to lower heat input, laser deposits showed numerous lack of fusion defects between BM and deposit, and also between individual layers of deposit. Structure of MAG deposit included sporadic gas entrapped bubbles only. The temperature conditions in both technologies have a direct impact on the microhardness profile of weld deposits. Hardness of top layer in both deposits are about the same (670-680 HV 0.1), hardness of base material is 195 HV 0.1. Due to lower heat input and narrow HAZ, hardness in laser deposit dropped very soon under the surface, whereas in MAG deposit high hardness maintained several mm under the surface. Despite of identical base material and welding wire used, corrosion resistance of deposits is slightly lower compared to base material due to change in chemical composition in deposits by burning off some elements, namely Cr. Change of chemical composition and corrosion rate is more pronounced in MAG deposit ($r_{corrMAG}$=0.46 mmpy, $r_{corrLASER}$=0.31 mmpy, r_{corrBM}=0.29 mmpy). Judging by the

thickness of interface compact layer of dissolution products formed by immersion in melt processed in HPDC process, the resistance of MAG weld deposit against dissolution in melt is at the level of resistance of original mold material (compact layer thickness about 0.2 mm), whereas resistance of laser weld deposit is significantly higher (compact layer thickness about 0.025 mm). Wear resistance copied hardness results, high hardness of deposits resulted in higher abrasive wear resistance compared to bas material, higher resistance showed MAG deposit compared to laser technology. In all tests, laser cladding showed slightly better results however contains more internal defects.
Authors recommend MAG welding when depositing larger areas and needing more deposited thickness. The weld deposit should be multilayered and the individual layers should be deposited immediately after each other. Less invasive laser welding is also recommended for multi-layer deposition, for smaller areas and less thicknesses.

Acknowledgments: Authors are grateful for the support of experimental works by projects VEGA No. 1/0497/20 "Application of progressive technologies in the restoration of functional surfaces of products" and APVV-16-0359 "The utilization of innovative technology for repair functional surfaces of mold casting dies for castings in automotive industry".

REFERENCES

1. S. Jhavar, C. P. Paul, N. K. Jain: Engineering Failure Analysis, 34, 2013, 519-535. http://dx.doi.org/10.1016/j.engfailanal.2013.09.006
2. M. J. Anderson, K. McGuire, R. C. Zante, W. J. Ion, A. Rosochowski, J. W. Brooks: Journal of Materials Processing Technology, 213(1), 2013, 111–119., http://dx.doi.org/10.1016/j.jmatprotec.2012.09.002
3. R. Ebara, K. Kubota: Engineering Failure Analysis, 15(7), 2008, 881–893. https://doi.org/10.1016/j.engfailanal.2007.10.016
4. S. Chander, V. Chawla: Materials Today: Proceedings, 4(2), 2017, 1147-1157. https://doi.org/10.1016/j.matpr.2017.01.131
5. R. Markezic, I. Naglic, N. Mole, R. Sturm: Engineering Failure Analysis, 95, 2019, 171-180. https://doi.org/10.1016/j.engfailanal.2018.09.010
6. Y. F. Wang, Z. G. Yang: Wear, 265(5-6), 2008, 871-878. https://doi.org/10.1016/j.wear.2008.01.014
7. A. Persson, S. Hogmark, J. Bergström: Surface and Coatings Technology, 191(2-3), 2005, 216-227. https://doi.org/10.1016/j.surfcoat.2004.04.053
8. J. Brezinova, D. Draganovska, A. Guzanova, P. Balog, J. Vinas: Metals, 6(2), 2016, 36. https://doi.org/10.3390/met6020036
9. J. C. Lee, H. J. Kang, W. S. Chu, S. H. Ahn: CIRP Annals, 56(1), 2007, 577-580. https://doi.org/10.1016/j.cirp.2007.05.138
10. Ch. Chen, Y. Wang, H. Ou, Y. He, X. Tang: Journal of Cleaner Production, 64, 2014, 13-23. http://dx.doi.org/10.1016/j.jclepro.2013.09.014
11. J. Brezinová et al.: Metals, 9(11), 2019, 1232. https://doi.org/10.3390/met9111232
12. J. Brezinova, M. Dzupon, D. Jakubeczyova, M. Vojtko, A. Guzanova, J. Brezina: Analysis of the quality duplex coating in melt of Al-Si based alloy, In: *Annual International Conference on Materials Science, Metal & Manufacturing, Global Science & Technology Forum*, Singapore, 2018, p.108-112
13. J. Brezinova, J. Vinas, P.O. Maruschak, A. Guzanova, D. Draganovska, M. Vrabel: *Sustainable renovation within metallurgical production*, first ed., RAM–Verlag, Lüdenscheid, Germany, 2017, 215 p.
14. A. Suarez, A.M. Suarez, W.T. Preciado: Procedia Engineering, 100, 2015, 584-591. https://doi.org/10.1016/j.proeng.2015.01.408
15. Z. Hu, X. Qin, T. Shao: Procedia Engineering, 207, 2017, 2203-2208. https://doi.org/10.1016/j.proeng.2017.10.982
16. Y. Zhao, X. Shi, K. Yan, G. Wang, Z. Jia, Y. Heb: Journal of Materials Processing Technology, 262, 2018, 382-391. https://doi.org/10.1016/j.jmatprotec.2018.07.003
17. Y. Zhang, G. Chen, C. Zhou, Y. Jiang, P. Zhong, Sh. Li: Journal of Materials Processing Technology, 245, 2017, 309-317. http://dx.doi.org/10.1016/j.jmatprotec.2017.02.029
18. L. P. Borrego, J. T. B. Pires, J. M. Costa, J. M. Ferreira: Engineering Failure Analysis, 16(2), 2009, 596–607. https://doi.org/10.1016/j.engfailanal.2008.02.010
19. Ch. Vundru, S. Paul, R. Singh, W. Yan: Procedia Manufacturing, 26, 2018, 952-961. https://doi.org/10.1016/j.promfg.2018.07.122
20. M. Franz, J. Bliedtner, C. Haupt: Procedia Engineering, 69, 2014, 237-240. https://doi.org/10.1016/j.proeng.2014.02.227
21. D. Cong et al.: Optics and Laser Technology, 53, 2013, 1-8. https://doi.org/10.1016/j.optlastec.2013.04.024
22. D. Cong et al.: Optics and Lasers in Engineering, 54, 2014, 55-61. http://dx.doi.org/10.1016/j.optlaseng.2013.09.012
23. C. Navas, A. Conde, B. J. Fernandez, F. Zubiri, J. Damborenea: Surface and Coatings Technology, 194(1), 2005, 136-142. https://doi.org/10.1016/j.surfcoat.2004.05.002
24. P. Kattire, S. Paul, R. Singh, W. Yan: Journal of Manufacturing Processes, 20, 2015, 492-499. http://dx.doi.org/10.1016/j.jmapro.2015.06.018
25. R. Song, S. Hanaki, M. Yamashita, H. Uchida: Materials Science and Engineering A, 483–484, 2008, 343-345. https://doi.org/10.1016/j.msea.2006.10.207
26. O. Knotek, F. Löffler and B. Bosserhoff, PVD coatings for diecasting moulds: Surface and Coatings Technology, 62, 1-3, 1993, 630-634. https://doi.org/10.1016/0257-8972(93)90310-K
27. E. Capello, D. Colombo, B. Previtali: Journal of Materials Processing Technology, 164-165, 2005, 990-1000. https://doi.org/10.1016/j.jmatprotec.2005.02.075
28. S. Nevskii, V. Sarychev, S. Konovalov, A. Granovskii, V. Gromov: Journal of Materials Research and Technology, 9(1), 2020, 539-550. https://doi.org/10.1016/j.jmrt.2019.10.083
29. V. Gliha, P. Maruschak, T. Vuherer: Materials and Technology, 47(4), 2013, 441-446.
30. H. Zhu: *Dissolution rate and mechanism of metals in molten aluminium alloy A380*, Purdue University, Indiana, USA, 2014, Open Access Theses. 465, https://docs.lib.purdue.edu/open_access_theses/465
31. S. Xu, X. Chen, S. Konovalov: Effect of phase transition temperature and particle size on residual stresses and properties of laser cladding layer, In: *IOP Conf. Series: Materials Science and Engineering, Metallurgy 2017*, Novokuznetsk, Russia, 411, 2018, p. 1-8. https://doi.org/10.1088/1757-899X/411/1/012084